Magnetic anisotropy of thin Co and Ni films on diamond surfaces

Bernd Stärk,* Peter Krüger, and Johannes Pollmann
Institut für Festkörpertheorie, Westfälische Wilhelms-Universität Münster, D-48149 Münster, Germany
(Received 13 July 2011; revised manuscript received 20 October 2011; published 9 November 2011)

We present results of *ab initio* investigations of magnetic properties of Co and Ni multilayers on diamond surfaces. The generalized gradient approximation is used within the framework of noncollinear density-functional theory, and fully relativistic pseudopotentials are employed together with a basis set of Gaussian orbitals. The validity of this approach is demonstrated for freestanding transition-metal (TM) monolayers and TM monolayers on the Cu(001) surface. Our results for these test systems are in good agreement with respective literature data. We employ the approach to study up to six Co or Ni adlayers on (111) and (001) surfaces of diamond. These systems are characterized by a very small lattice mismatch of the constituents. We analyze the influence of the strong covalent bonds forming in these hybrid systems on the magnetic properties, focusing on the magnetic anisotropy. For Co multilayers on C(111), the anisotropy energies are quite large and show a weak dependence on the number of adlayers. For Co or Ni multilayers on C(001), on the other hand, these energies are an order of magnitude smaller but their dependence on adlayer thickness is much more pronounced. For the hybrid systems considered, we find configurations with noncollinear magnetization within a given layer or on different layers to be unstable.

DOI: 10.1103/PhysRevB.84.195316 PACS number(s): 75.70.Ak, 75.70.Cn, 75.30.Gw

I. INTRODUCTION

Magnetic anisotropy is a key property of ferromagnetic materials and plays a major role in many technological applications. In particular, magnetic anisotropy effects in ultrathin films and heterogeneous multilayer systems have received a lot of attention both in experimental as well as in theoretical studies.[1,2]

Although the physical origins of magnetic anisotropy have been known for a long time,[3] it took almost 50 years for the first theoretical investigations for bulk[4] and surface systems[5] to become available. This is due to the large numerical effort required to describe anisotropy effects properly, especially for bulk systems where anisotropy energies are of the order of a few μeV. For these reasons, investigations of the magnetic anisotropy in bulk systems remain problematic, even today. For multilayers and surface systems, on the other hand, anisotropy energies are larger by about three orders of magnitude, and there has been a multitude of studies on these systems (for an overview, see Ref. 6 and references therein).

Although most studies of anisotropy effects concentrate on purely metallic multilayer systems, there has been an increasing interest in the study of semiconductor-ferromagnet hybrid systems in recent years due to their technological potential in spintronics.[7,8] For example, Kosuth *et al.*[9] have investigated anisotropy effects of thin Fe adlayers on a GaAs surface, finding a strong influence of the chemical bonds at the interface on the magnetic anisotropy.

The magnetic anisotropy depends heavily on the atomic structure of a considered system,[2] particularly on the lattice mismatch and interface roughness. This makes a meaningful comparison between experiment and theory rather difficult. Therefore, it is essential that considered systems are well defined and show good structural compatibility. In a previous contribution,[10] we investigated hybrid systems consisting of Co multilayers on (001) and (111) diamond surfaces, which have a very small lattice mismatch between the constituents and are well suited in this respect. These systems form strong covalent bonds between the diamond substrate and the ferromagnetic adlayers, leading to large binding energies.

In this work, we study electronic and magnetic properties of metal-semiconductor hybrid systems. In particular, we analyze the impact of the covalent interface bonds on the magnetic properties of the systems, focusing on anisotropy effects. We also investigate the consequences of replacing Co by Ni adlayers on the magnetic properties of the hybrid systems. Since their lattice constants are very similar, the substitution of Co by Ni hardly affects the structural properties. The magnetic moments and anisotropy of the hybrid systems are considerably different, however.

The paper is organized as follows. In Sec. II, we give a short overview of noncollinear density-functional theory as implemented in our program. To check the validity of our approach, we compare our results for freestanding transition-metal monolayers as well as transition-metal monolayers on Cu(001) with results from the literature in Sec. III A. The results for one to six Co adlayers on the C(111)-(1×1) surface are presented in Sec. III B. We then change the substrate to C(001)-(1×1) and consider Co as well as Ni adlayers as adsorbates in Sec. III C. A short summary concludes the paper in Sec. IV.

II. METHODOLOGY

Our calculations are carried out in the framework of density-functional theory employing pseudopotentials together with a basis set of atom-centered Gaussian orbitals of s, p, d, and s^* symmetry. Surfaces are simulated within the standard supercell approach using a slab geometry for the hybrid systems.

In a system with noncollinear magnetization, the energy can be written as a functional $\widetilde{E}$ of the Hermitian 2×2 density matrix $\varrho(\boldsymbol{r})$.[11] One can directly map this matrix to the charge density $n(\boldsymbol{r})$ and the vector of the magnetization density $\boldsymbol{m}(\boldsymbol{r})$ using Pauli spin matrices. Each element of

$\varrho(\boldsymbol{r})$ is given by a sum involving the Kohn-Sham spinors $\boldsymbol{\psi}_j(\boldsymbol{r}) = (\psi_j^1(\boldsymbol{r}), \psi_j^2(\boldsymbol{r}))$. These spinors are obtained by solving a noncollinear version of the Kohn-Sham equation that can be formally derived as the nonrelativistic limit of relativistic density-functional theory:[12]

$$[(-\Delta + V_{\mathrm{Coul}} + V_{\mathrm{ext}})\boldsymbol{I}_2 + \boldsymbol{V}_{\mathrm{xc}} + V_{\mathrm{SO}}\boldsymbol{L}\cdot\boldsymbol{S}]\boldsymbol{\psi}_j = \epsilon_j\boldsymbol{\psi}_j. \quad (1)$$

Here, V_{Coul} and V_{ext} are the Coulomb and the external potential, respectively, which already appear in conventional density-functional theory and are diagonal in spin space. We note that the external potential contains the Darwin and the mass term. $\boldsymbol{I}_2$ is the 2×2 unit matrix in spin space. The other two terms are the exchange-correlation potential and the spin-orbit (SO) interaction, which are, in general, nondiagonal in spin space.

The 2×2 matrix of the exchange-correlation potential $\boldsymbol{V}_{\mathrm{xc}}$ is the functional derivative of the exchange-correlation energy E_{xc} with respect to the components of the density matrix. It depends on $n(\boldsymbol{r})$ and on the vector $\boldsymbol{m}(\boldsymbol{r})$. In the local-spin-density approximation (LSDA), E_{xc} is written as an integral over local exchange densities $\epsilon_{\mathrm{xc}}^{\sigma}(\boldsymbol{r})$, which depend only on the charge density and on the absolute value of the magnetization. Therefore, the noncollinear exchange potential $\boldsymbol{V}_{\mathrm{xc}}$ can be derived from the collinear case by locally rotating the spin quantization axis.[13] In the generalized gradient approximation (GGA), however, one can formulate noncollinear versions in various manners.[14] We use the approach as derived by Peralta *et al.*[15] and the Perdew-Burke-Ernzerhof (PBE) formulation of the GGA.[16] For the local density approximation (LDA), we use the data of Ceperley and Alder[17] in the parametrization of Perdew and Zunger.[18]

In our approach, we replace the external potential V_{ext} and the spin-orbit potential $V_{\mathrm{SO}}\boldsymbol{L}\cdot\boldsymbol{S}$ by a sum over j-dependent pseudopotentials[19,20] with $j = l \pm 1/2$. These pseudopotentials are generated for the respective atoms according to the prescription of Hamann,[21] including nonlinear core corrections,[22] and they are eventually converted to the Kleinman-Bylander form[23] V_j^{KB} to improve the numerical efficiency of the calculations. For both steps, we use the atomic pseudopotential engine as described by Oliveira *et al.* in Ref. 24. In our calculation, orbital angular momenta up to $l = 2$ are included. As the spin-orbit interaction is usually small, it is advantageous to split the j-dependent atomic pseudopotential into a scalar-relativistic and a spin-orbit part:[20]

$$\begin{aligned} V_l^{\mathrm{SR,KB}} &= \frac{1}{2l+1}\left[(l+1)V_{l+1/2}^{\mathrm{KB}} + lV_{l-1/2}^{\mathrm{KB}}\right], \\ V_l^{\mathrm{SO,KB}} &= \frac{2}{2l+1}\left[V_{l+1/2}^{\mathrm{KB}} - V_{l-1/2}^{\mathrm{KB}}\right]. \end{aligned} \quad (2)$$

Both contributions are fitted to Gaussian functions[19] and transferred to the solid, leading to a nonlocal operator that is also nondiagonal in spin space (see Ref. 20 for details). For a Gaussian basis set, the resulting matrix elements have the same form as the overlap integrals, which are easily evaluated analytically.[25]

A fine real-space mesh is needed to represent the charge density since the pseudopotentials for transition metals are rather hard. To evaluate the charge density, we use the very efficient algorithms presented by Wieferink *et al.*[26] The decay constants[27] of the Gaussian basis functions are chosen so as to minimize the total energy in a calculation of the standard bulk configuration of the considered atomic species (for example, fcc bulk Ni for a Ni pseudopotential) and of appropriate monolayers. To circumvent numerical instabilities during the optimization of the decay constants, we employ the methods presented by Petersson *et al.*[28]

As pointed out by Jansen,[29] the Coulomb part of the total energy $\widetilde{E}$ should also include a relativistic correction (the so-called Breit interaction in Hartree form), which can be approximated by a dipole sum,[4]

$$E^{\mathrm{dipole}} = \frac{1}{c^2}\sum_{\tau\tau'}{}' \frac{1}{|\boldsymbol{\tau}-\boldsymbol{\tau}'|^3} \times\left[\boldsymbol{m}_\tau\boldsymbol{m}_{\tau'} - 3\frac{[(\boldsymbol{\tau}-\boldsymbol{\tau}')\cdot\boldsymbol{m}_\tau][(\boldsymbol{\tau}-\boldsymbol{\tau}')\cdot\boldsymbol{m}_{\tau'}]}{|\boldsymbol{\tau}-\boldsymbol{\tau}'|^2}\right], \quad (3)$$

in units of Rydberg (where $1/c = \alpha/2$ and α is the fine-structure constant).

This dipole sum can be evaluated very efficiently by methods based on the Ewald-Kornfeld approach[30,31] employing mixed real-space/Fourier-space techniques. We use the summation method as described in Ref. 32. In our program, the magnetic moment $\boldsymbol{m}_\tau$ localized at the position $\boldsymbol{\tau}$ is obtained by a Mulliken analysis[33] after the self-consistency cycle is finished. The resulting dipole sum is then added to the total energy, i.e., $E = \widetilde{E} + E^{\mathrm{dipole}}$.

The total energy of a system depends on the magnetic moments via the exchange-correlation potential, the spin-orbit potential, and the dipole energy. Assuming a collinear magnetic configuration, the exchange-correlation energy does not depend on the orientation of the magnetic moments with regard to the crystal axis. For the spin-orbit interaction and the dipole energy, this is usually not the case. For magnetic systems, these interactions lead to a dependence of the total energy on the direction of the magnetic moments. The energy difference between two magnetic orientations $\boldsymbol{m}_1(\boldsymbol{r})$ and $\boldsymbol{m}_2(\boldsymbol{r})$ is called magnetocrystalline anisotropy (MCA) energy, $E_{\mathrm{MCA}} = E_{\mathrm{MCA}}^{\mathrm{SO}} + E_{\mathrm{MCA}}^{\mathrm{dipole}}$. It consists of $E_{\mathrm{MCA}}^{\mathrm{SO}} = \widetilde{E}[\boldsymbol{m}_1(\boldsymbol{r})] - \widetilde{E}[\boldsymbol{m}_2(\boldsymbol{r})]$ resulting from the difference of the total energies $\widetilde{E}$ including the spin-orbit interaction, and $E_{\mathrm{MCA}}^{\mathrm{dipole}}$ resulting from the respective difference of the dipole interaction energies E^{dipole} for both configurations.

Integrations over the Brillouin zone are performed using special **k**-point sets according to the prescription of Monkhorst and Pack.[34] To obtain reliable results for spin polarization, as well as magnetization, a precise sampling of the Fermi surface is mandatory. As all systems considered in this work are metallic, we employ the extended broadening scheme introduced by Methfessel *et al.*[35] The number of **k** points and the broadening width η depend on the required accuracy of the Brillouin-zone integrals. An exact solution requires $\eta \to 0$ and $N_k \to \infty$, which is of course not feasible due to computational limitations. Therefore, one has to choose an acceptable compromise. This point will be addressed in some more detail at the end of Sec. III A.

III. RESULTS

In this section, we first demonstrate the usefulness of our approach by presenting magnetic moments and anisotropy energies of free and adsorbed transition-metal (TM) monolayers in comparison with literature data. Then we turn to the main subject of our contribution and discuss thin TM films on diamond surfaces and the influence of an insulating substrate on their magnetic behavior.

A. Transition-metal monolayers

Freestanding TM monolayers, as well as TM monolayers adsorbed on the Cu(001) surface, are especially suitable prototype systems for a comparison of our results with literature data since these systems have been studied extensively in the past.

We address freestanding Fe, Co, and Ni fcc monolayers, which have a very simple structure because there is only one atom per square unit cell. In addition, we present results for these monolayers adsorbed on Cu substrates consisting of three Cu(001) layers. All calculations (including those for the freestanding monolayers) have been performed at the experimental bulk lattice constant $a_{\mathrm{exp}} = 3.60$ Å of Cu leading to a surface lattice constant of $a_{001} = 2.54$ Å. The TM/Cu systems have been relaxed in the direction perpendicular to the surface until all forces are smaller than 1 mRy/a_B.

To ensure a high accuracy in the determination of the magnetic moments and the anisotropy energies, we have used a very fine **k**-point mesh of $84 \times 84\mathbf{k}$ points in the whole 2D Brillouin zone. As all systems are metallic, we employ the Methfessel-Paxton broadening scheme[35] of second order with a very small width of 1.5meV.

In Table I, we present the magnetic moments of freestanding and adsorbed TM monolayers, as resulting from our LDA and GGA calculations, in comparison with literature data. We note in passing that the *absolute* value of the magnetic moment hardly depends on the direction of the magnetization or on the spin-orbit interaction. In the case of a Co monolayer, for example, the difference between a calculation including the SO interaction (with $\boldsymbol{m} \parallel \boldsymbol{e}_z$) to one neglecting this interaction is less than $0.01\mu_B$.

TABLE I. Magnetic moments μ (in μ_B/atom) of freestanding Fe, Co, and Ni monolayers, and of these monolayers adsorbed on a Cu(001) surface. The experimental lattice constant of Cu is used, and spin-orbit interaction is taken into account.

	LDA		GGA	
	this work	Lit.	this work	Lit.
Fe(ML)	3.13	3.00[a]	3.13	2.97[b]
Co(ML)	2.11	2.09[a]	2.11	2.07[b]
Ni(ML)	0.98	1.00[a]	0.99	0.98[b]
Fe/Cu(001)	2.76	2.85[c]	2.85	2.78[b]
Co/Cu(001)	1.78	1.72[d]	1.84	1.83[b]
Ni/Cu(001)	0.34		0.49	0.44[b]

[a]Reference 6.
[b]Reference 36.
[c]Reference 37.
[d]Reference 38.

The magnetic moments for the monolayers are considerably higher than the respective GGA bulk values for Fe ($2.19\mu_B$), Co ($1.63\mu_B$), and Ni ($0.64\mu_B$). This is due to the lower coordination of the atoms in a monolayer as compared to the bulk crystal. For a TM layer on a substrate consisting of three Cu(001) layers, the magnetic moment is always strongly localized at the respective magnetic adlayer atoms, whereas the Cu atoms have a negligible magnetic moment that always amounts to less than $0.02\mu_B$ per atom. The magnetic moments of the ferromagnetic top atoms are reduced in comparison to those of the freestanding monolayers due to the presence of the Cu substrate and the concomitant increased coordination. Comparing our results with the literature data in Table I, we note that for both the monolayers as well as the TM/Cu systems, the magnetic moments agree within a few percent with theoretical results from plane-wave[36] and full-potential linear augmented plane-wave[6,37,38] calculations. The magnitude of the magnetic moments hardly depends on the used functional. This can be attributed to the fact that the lattice constants are the same in both calculations.

Magnetocrystalline anisotropy energies, on the other hand, are much more sensitive to calculational details. Therefore, they are a very meaningful test for the accuracy and stability of our approach. In Table II, we present the spin-orbit part of the MCA energy

$$E_{\mathrm{MCA}}^{\mathrm{SO}} = \widetilde{E}(\boldsymbol{m} \parallel \boldsymbol{e}_x) - \widetilde{E}(\boldsymbol{m} \parallel \boldsymbol{e}_z) \tag{4}$$

for the freestanding monolayers and TM/Cu systems. In addition to calculating the anisotropy energies fully self-consistently, we have also employed the force theorem (FT)[4] for their evaluation. In the latter approach, one calculates the MCA energies as the difference between the band-structure energies for both magnetic configurations. In this case, there is no need to converge a complete self-consistency cycle.

The first point to notice in Table II is the good agreement between the MCA energies calculated using the force theorem with those determined self-consistently. This can be attributed to the small magnitude of the spin-orbit interaction in these ferromagnets compared to the other terms in the Hamiltonian. This point is further confirmed by the fact that a self-consistent calculation starting from a potential determined without

TABLE II. Spin-orbit part of the MCA energy of Fe, Co, and Ni monolayers and of these monolayers adsorbed on a Cu(001) surface. Results obtained using the force theorem or self-consistent-field calculations are labeled FT and SCF, respectively. The experimental lattice constant of Cu is used in all calculations.

	LDA			GGA		
	FT	SCF	Lit.[a]	FT	SCF	Lit.[a,b]
Fe	0.50	0.57	0.21[a]	0.63	0.65	+0.50,[a] + 0.63[b]
Co	−1.40	−1.42	−1.42[a]	−1.39	−1.33	−1.49,[a] − 1.26[b]
Ni	−2.08	−2.01	−1.64[a]	−0.89	−0.77	−0.77,[a] − 1.43[b]
Fe/Cu	0.28	0.29		0.38	0.38	+0.29[b]
Co/Cu	−0.30	−0.34		−0.57	−0.52	−0.23[b]
Ni/Cu	−0.77	−0.74		−1.02	−1.02	−1.24[b]

[a]Reference 6.
[b]Reference 36.

spin-orbit interaction takes only three to five iterations to converge. Thus for interface and surface systems, it may often be sufficient to employ the force theorem, as has been noticed previously.[39] Nevertheless, for the new systems to be reported about in the remainder of this work, we prefer to carry out all calculations self-consistently.

For Fe and Fe/Cu, we find the energetically most favorable configuration to be the one in which the magnetic moments point out-of-plane, whereas for Co and Ni they prefer to point in-plane. This general behavior is in excellent agreement with previous theoretical results.[6,36] On a more quantitative basis, several agreements but also some discrepancies are to be noted. For the freestanding Ni monolayer, e.g., where previous GGA results of other groups show a large scatter by about a factor of 2, our result agrees with that of Ref. 6 while it deviates by some 0.7meV from the result of Ref. 36. This shows the high sensitivity of the magnetic anisotropy to numerical details. This notion is further corroborated by the MCA energies of the freestanding Fe and Co monolayers. While the GGA results for the Fe monolayer and both the LDA and GGA results for the Co monolayer are in very reasonable agreement, our LDA results for the Fe monolayer show a rather large deviation from the results of Ref. 6.

Next, we want to identify the influence of the employed exchange-correlation (XC) functionals on the anisotropy energies by comparing respective results in Table II. For Fe and Co monolayers, we obtain very similar anisotropy energies for both LDA and GGA functionals as long as we fix the lattice constant to the experimental lattice constant of Cu. The MCA energy for a Ni monolayer, on the other hand, shows quite a sizable dependence on the employed functional, as has been noted previously.[6] For the TM/Cu systems, the LDA anisotropy energies are always smaller than the respective GGA values. So there is no unique or systematic trend to be noted concerning the influence of the XC functional on the MCA energy.

We note in passing that the magnitude of the magnetic moment is only a minor indicator of the magnetic anisotropy energy. In fact, the MCA energy depends more strongly on details of the band structure and on the shape of the Fermi surface than on the exchange splitting, as has been shown previously.[1] For example, the Fe monolayer has the smallest anisotropy energy of the three transition-metal monolayers but the largest magnetic moment, confirming this notion.

In addition to the SO interaction, the dipole-dipole interaction can also contribute significantly to the total anisotropy energy (see Table III). For the Fe monolayer and the Fe/Cu system, the SO and dipole contributions to the total MCA energy are of the same order (see, e.g., the LDA values of $0.57/-0.21$ meV for the Fe monolayer and $0.29/-0.17$ meV for the Fe/Cu system, respectively), whereas for freestanding Co and Ni monolayers, as well as for Co and Ni monolayers on Cu, the dipole interaction is much less important. This results from the fact that the size of the dipole contribution depends approximately quadratically on the magnetic moment. Nevertheless, these contributions have to be taken into account, especially when adding further ferromagnetic adlayers. In general, the dipole part of the magnetic anisotropy favors magnetic moments to be in-plane. As a consequence, the total magnetic anisotropy energy is increased by the dipole contribution for Co and Ni while it is decreased considerably for Fe.

TABLE III. Self-consistent spin-orbit (SO) and dipole-dipole (dipole) contributions to the total MCA energy (total) (in meV). For further details, see the caption of Table II.

	LDA			GGA		
	SO	dipole	total	SO	dipole	total
Fe	0.57	−0.21	0.36	0.65	−0.21	0.44
Co	−1.42	−0.10	−1.52	−1.33	−0.10	−1.43
Ni	−2.01	−0.02	−2.03	−0.77	−0.02	−0.79
Fe/Cu	0.29	−0.17	0.12	0.38	−0.19	0.19
Co/Cu	−0.34	−0.07	−0.41	−0.52	−0.08	−0.60
Ni/Cu	−0.74	−0.00	−0.74	−1.02	−0.00	−1.02

At this point, we briefly address the *convergence of our calculations*. We would like to emphasize that a precise sampling of the Brillouin zone turns out to be a necessary prerequisite for a reliable description of magnetic properties, especially of MCA energies. To illustrate this point, we present the spin-orbit contribution to the MCA energy of a freestanding Co monolayer calculated on the basis of the force theorem within the LDA for different numbers of **k** points N_k and different Gaussian broadenings η (Fig. 1).

For larger systems, the determination of eigenvalues becomes the most time-consuming part of the calculations. In a Gaussian basis set, however, the size of the Hamiltonian matrices is rather small, as compared to a plane-wave basis set, allowing for a rapid solution of the eigenvalue problems. Nevertheless, it is highly desirable to reduce the number of **k** points as much as possible. As can be seen from Fig. 1(a), convergence with respect to the number of **k** points depends strongly on the broadening width η. A large broadening η can speed up the convergence of the Brillouin zone integrals considerably, leading, however, to a large error in the anisotropy energy. For example, the anisotropy energy determined with $\eta = 100$ meV differs from the one determined for $\eta = 0.1$meV by some 0.2meV. However, anisotropy energies determined for $\eta \leqslant 1$ meV differ by less than a few μeV from each other. Therefore, the broadening width should be of this magnitude.

Comparing Figs. 1(a) and 1(b), we find that the use of extended broadening techniques according to Ref. 35 does not speed up the convergence of the integrals with respect to the number of **k** points, but it does reduce the dependence on the broadening width η. Therefore, we use this extended scheme throughout the paper.

Figure 1(b) suggests that about 7000 sampling points in the Brillouin zone are necessary to obtain an accuracy of some μeV for $\eta = 1$ meV. This amount of accuracy is sufficient for all surface and interface systems considered here, and this grid is used in the remainder of this work.

B. Co multilayers on the C(111) surface

In the following, we apply our approach to metal-semiconductor hybrid systems. This class of systems has attracted much attention in recent years due to its possible application in spintronic devices.[7–9] In particular, Co

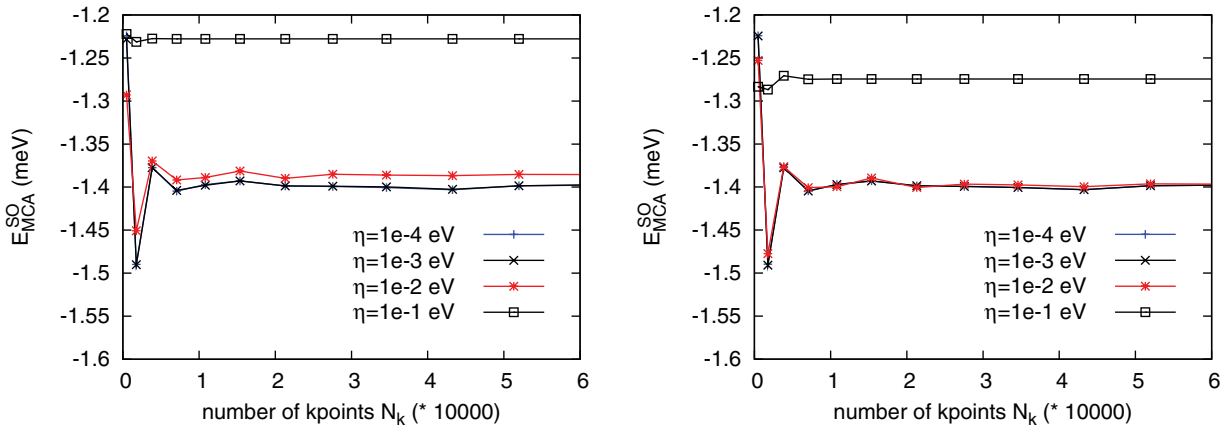

FIG. 1. (Color online) Spin-orbit part $E^{\mathrm{SO}}_{\mathrm{MCA}}$ of the magnetic anisotropy energy of a Co monolayer in dependence on the number of **k** points N_k in the Brillouin zone for different broadening widths η. In (a), Gaussian broadening ($n = 0$) is used, while in (b), second-order broadening ($n = 2$) according to Ref. 35 is used.

multilayers on graphite surfaces[40] or on graphene[40,41] have been studied in the context of spin valves and graphene-based spintronic devices. Quite generally, the magnetic properties of such systems depend strongly on the nature of the interface bonds. We illustrate this point by investigating Co multilayers on C(111) in this section. Afterwards, we study Co multilayers on a C(001) surface and discuss the importance of the surface topology on the magnetic properties. Subsequently, we replace the Co by Ni adlayers and explore the concomitant effects in the magnetic anisotropy of the resulting Ni:C(001) systems.

1. Structural properties of Co:C(111) systems

A useful hybrid system must have a good structural compatibility because a large lattice mismatch leads to diffusive transport processes, as has been shown previously.[42] These quickly destroy the magnetization of the currents induced by the source. To this end, we recently[10] proposed a hybrid system consisting of n Co adlayers on a diamond (111) surface. We will henceforth refer to this system as n Co:C(111).

The experimental bulk lattice constant of Co is $a = 2.51$ Å for the hcp structure with an optimal c/a ratio of 1.62. This lattice constant shows an almost perfect matching (mismatch of less than 1%) with the surface lattice constant $a_{C(111)} = 2.52$ Å of C(111)-(1×1). Therefore, the constituents of this metal-semiconductor hybrid system are highly compatible. Our calculated GGA bulk lattice constant of hcp Co amounts to $a = 2.52$ Å and is thus only 0.4% larger than the experimental value. For diamond, the calculated lattice constant of 3.57 Å yields $a_{C(111)} = 2.52$ Å, in full agreement with experiment. Thus the theoretical lattice mismatch of <0.2% is even smaller than in experiment. Therefore, we use the theoretical GGA lattice constant of diamond for the hybrid systems.

We briefly summarize the structural and electronic properties of this hybrid system. For a more detailed discussion of its structure, we refer the reader to Ref. 10. Starting with one Co adlayer on C(111), the energetically most favorable adsorption configuration turns out to be the one shown in Fig. 2. The Co adatoms are located above the surface layer C atoms in *on-top* positions saturating all dangling bonds of the substrate. They form strong covalent Co-C hybrid bonds, which lead to a large binding energy of 1.9 eV per Co atom.

Due to the negligible lattice mismatch between diamond and hcp cobalt, Co atoms adsorb in hcp bulk Co sites characteristic for a Co(0001) surface when adding further

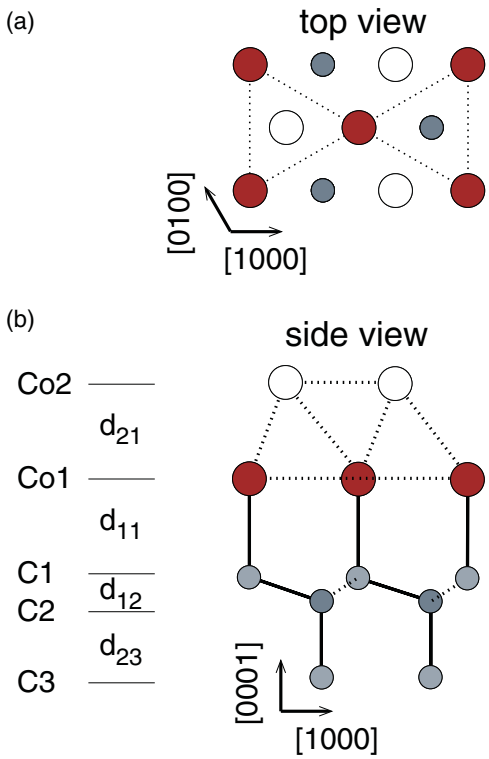

FIG. 2. (Color online) Top and side view of one and two Co adlayers on the C(111) surface (see text). Large filled red circles mark Co atoms on the first adlayer and large open circles mark Co atoms on the second adlayer. Small blue circles indicate C substrate atoms. Full lines represent covalent sp^3 or pd bonds parallel to the drawing plane, while dashed lines represent sp^3 bonds that form an angle with the drawing plane or metallic dd bonds. In the top view, only dd bonds between Co atoms on the first adlayer are indicated by dashed lines.

adlayers. For 2 Co:C(111), the most favorable configuration for the top Co layer is also shown in Fig. 2 (open circles). For a larger number of Co adlayers, we find that the interface has only a minor impact on the structural properties of both the Co layers and the diamond substrate. For the Co adlayers, we observe some inward relaxations with respect to bulk Co sites, while the structure of the diamond substrate layers is hardly changed in comparison to bulk diamond.

2. *Magnetic properties of Co adlayers on C(111)*

Although the structural properties away from the interface are only slightly influenced, the interface hybrid bonds between the substrate and the Co adlayers have a large impact on both the magnetic moments as well as on the anisotropy properties of the systems. In Table IV, we present the magnetic properties for one to six Co adlayers on the C(111) surface. The magnetic anisotropy energies are split into spin-orbit and dipole contributions. For 1 Co:C(111), the value of the magnetic moment ($0.94\mu_B$) is rather small in comparison to the bulk value of $\mu_{\rm hcp} = 1.62\mu_B$ due to the covalent nature of the Co-C bond. The rather small magnetic moment leads to a negligible dipole anisotropy of only -0.03 meV. Yet there is an appreciable spin-orbit anisotropy energy of 0.62 meV favoring the direction of the magnetic moment to be out-of-plane eventually. These findings are in strong contrast to the respective results for a freestanding hcp Co monolayer, for which the magnetic moment amounts to $\mu_{\rm mono} = 1.95\mu_B$ and the total magnetic anisotropy energy amounts to -0.43 meV. Thus, the presence of the diamond substrate changes the easy axis of magnetization from in-plane to out-of-plane and increases the absolute value of the magnetic anisotropy energy by about 50%, although the magnetic moment is reduced significantly. As the unit cell is hexagonal, there is also a small energy difference between different in-plane configurations. These energy differences are about two orders of magnitude smaller than the energy difference between an out-of-plane and an in-plane configuration and are therefore neglected. Again, one can observe that the magnetic moment is only a minor indicator of the magnitude of the anisotropy energy.

The addition of more Co adlayers to the system leads to an increase of the average magnetic moments since every Co adatom carries an additional magnetic moment. An analysis shows, however, that the magnetic moments at the interface are always reduced ($<1\mu_B$) with respect to the bulk value of $\mu_{\rm hcp} = 1.63\mu_B$, whereas the top Co atom always has an increased magnetic moment of $\mu_{\rm top} \approx 1.7\mu_B$.

TABLE IV. Average magnetic moments $\mu_{\rm tot}/n$ (in μ_B per Co atom), as well as spin-orbit and dipole contributions to the total anisotropy energy $E_{\rm MCA}$ (in meV) for n Co:C(111).

n	$\mu_{\rm tot}/n$	$E^{\rm SO}_{\rm MCA}$	$E^{\rm dip}_{\rm MCA}$	$E_{\rm MCA}$
1	0.94	0.62	−0.03	0.59
2	1.46	0.42	−0.13	0.29
3	1.44	0.41	−0.20	0.21
4	1.53	0.30	−0.29	0.01
5	1.52	0.45	−0.36	0.09
6	1.55	0.56	−0.44	0.12

The spin-orbit anisotropy part shows only a slight variation when adding further ferromagnetic layers to the surface. This weak dependence of the anisotropy energy on the number of adlayers is rather rare, and for most other systems this dependence is strong. It is very difficult to trace this peculiar behavior back to its physical origins, as magnetic anisotropy energies depend on the band structure as a whole and on the concrete shape of the Fermi surface.[1] Nevertheless, for freestanding Fe monolayers[43] and Fe monolayers on MgO (Ref. 44), the contribution of specific bands to the anisotropy energy has been assigned successfully. In our case, however, the band structures are very intricate, particularly for more than one ferromagnetic adlayer. Thus, a corresponding analysis turned out to be less revealing.

The dipole interaction, on the other hand, can be understood much more easily. Adding additional layers of Co to the surface leads to an almost linear increase in the magnetic anisotropy energies. This thickness dependence of the anisotropy has been observed previously[45] and can be ascribed to long-range parts of the dipole-dipole interaction, namely the volume contribution of the shape anisotropy known from continuum electrodynamics. The dipole interaction usually prefers an in-plane orientation of the magnetic moments and thus counteracts the magnetic anisotropy stemming from the spin-orbit interaction. Eventually, the dipole part exceeds the spin-orbit part and the preferred magnetic orientation switches to in-plane.

3. *Noncollinear configurations*

For more than one adlayer of Co, it is also conceivable that the magnetic moments located at different Co atoms of one layer or at different layers point in different directions. Such configurations have been observed, for example, by Hobbs *et al.*[46] for Cr on Cu(111) surfaces in a $\sqrt{3} \times \sqrt{3}$ reconstruction. Also, noncollinear structures have been proposed by Meyerheim *et al.*[47] to explain the observed magnetic behavior of ultrathin Fe layers on the Cu(001) surface. Using DFT they find quasistable noncollinear configurations explaining the vanishing total magnetic moment of this particular system. In these configurations, the magnetic moments in each ferromagnetic adlayer point in the same directions, but the directions differ from layer to layer. In all cases, these quasistable structures have a higher energy than collinear configurations, in agreement with previous studies.[48] In our case, however, these noncollinear configurations are not stable as they converge to a purely collinear magnetic structure during the self-consistency cycle. As an example, we present the evolution of the magnetic moments for 3 Co:C(111) in Fig. 3. At the beginning of the calculations, the magnetic moment on the top Co layer is parallel to the surface normal, that of the second Co layer points in-plane, and the one on the bottom Co layer is antiparallel to the surface normal. In the following, we refer to this configuration as $\Uparrow\Rightarrow\Downarrow$. During the self-consistency cycle, the angles between the local magnetic moments and the surface plane converge to a common angle of about 20° with respect to the surface plane for all three layers. The resulting magnetic configuration represents a stable energy minimum, which is 0.5 meV per unit cell higher

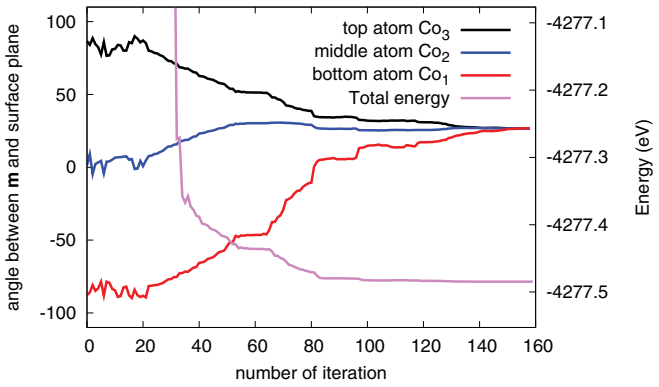

FIG. 3. (Color online) Evolution of the angle between the localized magnetic moments and the surface plane for the 3 Co:C(111) system during the self-consistency cycle. The starting configuration is $\Uparrow, \Rightarrow, \Downarrow$ from top to bottom adlayer.

than the (global) minimum $\Uparrow\Uparrow\Uparrow$ presented in the preceding section.

We have also considered numerous other starting configurations (for example, $\Uparrow\Uparrow\Downarrow$ and $\Rightarrow\Uparrow\Downarrow$), none of which has proven to lead to a stable noncollinear configuration. This is due to the fact that the system prefers collinear magnetic configurations because these reduce the exchange energy of the system. During the self-consistency cycle, the system reacts by aligning the noncollinear magnetic moments. Obviously, the spin-orbit interaction is not strong enough to counteract this effect, as it is roughly two orders of magnitude smaller than the exchange interaction.

C. Co and Ni multilayers on the C(001) surface

1. *Structural properties of Co:C(001) and Ni:C(001) systems*

The second kind of hybrid system considered in this work consists of n Co or Ni adlayers adsorbed on a C(001) substrate surface. Henceforth, we refer to these systems as n Co:C(001) and n Ni:C(001), respectively.

For n Co:C(001), the structural properties have also been discussed at length in Ref. 10. In the energetically most favorable configuration, the Co atoms reside in ideal diamond-lattice positions above the substrate (see Fig. 4) saturating all dangling bonds of the substrate surface by forming two covalent Co-C bonds per unit cell. Due to these two bonds, the binding energy of the Co adlayer is very large, amounting to 3.3 eV per unit cell. Additional Co adlayers can adsorb in ideal Co(001) positions since the mismatch between the C(001) and fcc cobalt surface lattice constants is again smaller than 1%. For the top Co adlayers, there is some inward relaxation comparable to that of the n Co:C(111) case, while the diamond substrate is again hardly affected.

As fcc Ni has a lattice constant close to the value of fcc Co ($a_{\mathrm{Ni}}^{\mathrm{exp}} = 3.52$ Å and $a_{\mathrm{Co}}^{\mathrm{exp}} = 3.54$ Å , respectively), one can replace the Co atoms by Ni atoms in the above structure without a significant increase in the lattice mismatch (cf. Ref. 49 for details). This allows us to investigate the influence of an additional d electron per atom in the transition-metal adlayers on the magnetic properties of the system without disturbing structural differences since the atomic structures are very similar to those of n Co:C(001). The Ni adlayers also

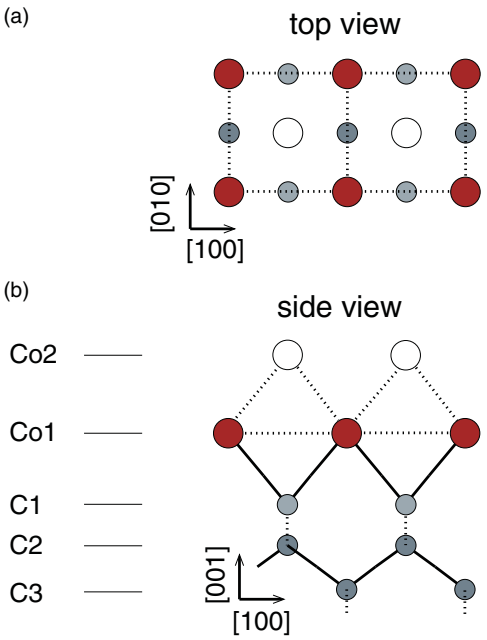

FIG. 4. (Color online) Top and side view of one and two Co layers on the C(001) surface. For further details, see the caption of Fig. 2.

show a similar inward relaxation to that of the Co adlayers, and the structure of the C(001) substrate surface is again hardly affected by the presence of the adlayers.

2. *Magnetic properties of Co adlayers on C(001)*

The magnetic moment at the interface is again strongly influenced by the covalent bonds forming at the interface. They quench μ_{tot} of the 1 Co:C(001) system to $0.44\mu_B$ (see Table V). An analysis of the moments on each of more than one Co adlayer (cf. Ref. 10) shows that the magnetic moments at the interface remain smaller than $1.0\mu_B$ and those on the inner layers of the adsorbed thin films quickly converge to the bulk value of $\mu_{\mathrm{fcc}} = 1.68\mu_B$. The magnetic moments of the top-layer atoms are again increased with respect to their bulk values and amount approximately to $1.9\mu_B$ for all systems. The average moments are similar to those of the n Co:C(111) system except for the 1 Co:C(001) case.

Table V also shows the MCA energies of the systems. We find that the magnetic anisotropy stemming from the spin-orbit interaction is about an order of magnitude smaller than that in the case of n Co:C(111) and prefers the magnetic moment to be out-of-plane. The only exception is 1 Co:C(001), where the preferred axis is in-plane but with a very small anisotropy

TABLE V. Same as Table IV but for n Co:C(001).

n	μ_{tot}/n	$E_{\mathrm{MCA}}^{\mathrm{SO}}$	$E_{\mathrm{MCA}}^{\mathrm{dip}}$	E_{MCA}
1	0.44	−0.01	−0.01	−0.02
2	1.42	0.01	−0.12	−0.11
3	1.47	0.04	−0.20	−0.16
4	1.53	0.08	−0.28	−0.20
5	1.55	0.11	−0.36	−0.25
6	1.58	0.03	−0.45	−0.42

TABLE VI. Same as Table V but for n Ni:C(001).

n	μ_{tot}/n	$E_{\text{MCA}}^{\text{SO}}$	$E_{\text{MCA}}^{\text{dip}}$	E_{MCA}
1	0.00	0.00	0.00	0.00
2	0.44	−1.52	−0.01	−1.53
3	0.40	−0.08	−0.02	−0.10
4	0.47	−0.28	−0.03	−0.31
5	0.47	−0.17	−0.04	−0.21
6	0.53	−0.47	−0.06	−0.53

energy. However, this part is exceeded by the dipole part of the anisotropy, which is dominant for each system with more than one Co adlayer. Thus the easy magnetic axis of the system is always in-plane, contrary to the Co:C(111) system.

3. *Magnetic properties of Ni adlayers on C(001)*

For n Ni:C(001) systems, the additional d electron per adlayer atom has a significant influence on the magnetic properties of the system (see Table VI). In general, the magnetic moments of Ni systems are smaller than those for Co systems. For a free Ni atom, the magnetic moment is only $2\mu_B$ due to Hund's rule, while it is $3\mu_B$ for a Co atom. For fcc bulk Ni, our calculated magnetic moments are also about $1\mu_B$ smaller than the respective value for fcc Co and amount to $0.60\mu_B$, in good agreement with experiment[50] ($\mu_{\text{exp}} = 0.61\mu_B$).

This has some significant consequences for fcc Ni on the C(001) surface. For one adlayer of Ni, the two covalent bonds render the whole system unmagnetic, although the structural properties remain almost unchanged in comparison to 1 Co:C(001). For two Ni adlayers, an analysis of the localized magnetic moments shows a small magnetic moment at the interface Ni atoms ($\mu_{\text{interface}} = 0.21\mu_B$) while the magnetic moments of the Ni atoms at the surface ($\mu_{\text{surface}} = 0.64\mu_B$) are of the same magnitude as in the bulk. The small magnetic moment for the interface Ni layer, however, vanishes for more than two Ni adlayers, leading to a magnetic "dead" Ni layer at the interface. Thus, the additional d electron present in Ni leads to significantly changed magnetic properties in comparison to the Co:C(001) system.

Of course, the vanishing magnetic moment for 1 Ni:C(001) leads to a vanishing magnetic anisotropy energy. For 2 Ni:C(001), there is a large anisotropy energy of −1.53 meV that even exceeds the (GGA) anisotropy energy of a free-standing Ni monolayer. For more than two Ni adlayers, the anisotropy energies return to the same magnitude as in the n Co:C(001) systems. As magnetic moments of this system are about $1\mu_B$ smaller than for systems containing Co, the dipole part of the anisotropy is very small and the anisotropy energies are dominated by the spin-orbit contribution.

IV. SUMMARY

In summary, we have investigated magnetic properties of ferromagnet-semiconductor hybrid systems in the framework of noncollinear density-functional theory employing the generalized gradient approximation. We have considered up to six Co adlayers on C(111) and up to six Co or Ni adlayers on C(001) surfaces, respectively. It turns out that strong covalent bonds form between the diamond substrate surface layer and the first Co or Ni layer at the interface. These bonds distinctly quench the magnetic moments at the interface. The addition of further adlayers quickly reestablishes the bulk magnetic moments in the inner layers of the adsorbed TM films, while the moments at the interface remain to be considerably reduced and those at the top layer of the films are enhanced as compared to the bulk moments.

The spin-orbit contribution to the anisotropy energies is heavily influenced by the covalent interface bonds and depends strongly on the structural properties of both the substrate and the adsorbate. For n Co:C(111), the anisotropy energies depend only to a small extent on the number of adlayers as compared to the n Co:C(001) and n Ni:C(001) systems. For the latter, the anisotropy energies are much smaller and depend more strongly on the number of adlayers. Although changes in the atomic structure are only small when replacing Co by Ni, the magnetic moments and anisotropy energies of both systems differ noticeably. In general, these effects cannot be directly ascribed to certain atoms or bonds as they have their origin in a superposition of small changes in the band structure when changing the magnetic orientation of the sample. The dipole part of the anisotropy, on the other hand, can be understood much more easily in terms of volume anisotropy effects well known from continuum electrodynamics. Our calculations indicate, in general, that configurations with noncollinear magnetic moments within a given layer or in different adlayers are unstable for the kind of systems investigated.

*bernd.staerk@uni-muenster.de

[1] *Ultrathin Magnetic Structures*, edited by J. Bland and B. Heinrich (Springer-Verlag, Berlin, 1994), Vol. I.
[2] M. T. Johnson, P. J. H. Bloemen, F. J. A. den Broeder, and J. J. de Vries, Rep. Prog. Phys. **59**, 1409 (1996).
[3] J. H. van Vleck, Phys. Rev. **52**, 1178 (1937).
[4] G. H. O. Daalderop, P. J. Kelly, and M. F. H. Schuurmans, Phys. Rev. B **41**, 11919 (1990).
[5] J. G. Gay and R. Richter, J. Appl. Phys. **61**, 3362 (1987).
[6] R. Wu and A. J. Freeman, J. Magn. Magn. Mater. **200**, 498 (1999).
[7] I. Žutić, J. Fabian, and S. D. Sarma, Rev. Mod. Phys. **76**, 323 (2004).
[8] E. Sjöstedt, L. Nordström, F. Gustavsson, and O. Eriksson, Phys. Rev. Lett. **89**, 267203 (2002).
[9] M. Kosuth, V. Popescu, H. Ebert, and G. Bayreuther, Europhys. Lett. **72**, 816 (2005).
[10] B. Stärk, P. Krüger, and J. Pollmann, Phys. Rev. B **81**, 035321 (2010).
[11] L. M. Sandratskii, Adv. Phys. **47**, 91 (1996).

[12]E. Engel, Relativistic Density Functional Theory, in *Relativistic Electronic Structure Theory*, Part 1, edited by P. Schwerdtfeger, (Elsevier, Amsterdam, 2002), p. 523.
[13]U. von Barth and L. Hedin, J. Phys. C **5**, 1629 (1972).
[14]P. Kurz, F. Förster, L. Nordström, G. Bihlmayer, and S. Blügel, Phys. Rev. B **69**, 024415 (2004).
[15]J. E. Peralta, G. E. Scuseria, and M. J. Frisch, Phys. Rev. B **75**, 125119 (2007).
[16]J. P. Perdew, K. Burke, and M. Ernzerhof, Phys. Rev. Lett. **77**, 3865 (1996).
[17]D. M. Ceperley and B. J. Alder, Phys. Rev. Lett. **45**, 566 (1980).
[18]J. P. Perdew and A. Zunger, Phys. Rev. B **23**, 5048 (1981).
[19]G. B. Bachelet, D. R. Hamann, and M. Schlüter, Phys. Rev. B **26**, 4199 (1982).
[20]L. A. Hemstreet, C. Y. Fong, and J. S. Nelson, Phys. Rev. B **47**, 4238 (1993).
[21]D. R. Hamann, Phys. Rev. B **40**, 2980 (1989).
[22]S. G. Louie, S. Froyen, and M. L. Cohen, Phys. Rev. B **26**, 1738 (1982).
[23]L. Kleinman and D. M. Bylander, Phys. Rev. Lett. **48**, 1425 (1982).
[24]M. J. Oliveira and F. Nogueira, Comput. Phys. Commun. **178**, 524 (2008).
[25]P. Schröer, P. Krüger, and J. Pollmann, Phys. Rev. B **47**, 6971 (1993).
[26]J. Wieferink, P. Krüger, and J. Pollmann, Phys. Rev. B **74**, 205311 (2006).
[27]As decay constants, we use 0.18, 0.52, 1.42, 3.70, and 10.58 for Co; 0.22, 0.69, 1.80, 4.44, and 12.25 for Ni; 0.18, 0.58, 1.57, 3.95, and 10.77 for Fe; and 0.18, 0.47, 3.30, and 9.61 for Cu (in atomic units). For the C atoms, we use 0.25, 0.87, and 3.60, while a decay constant of 0.35 is employed for the saturating hydrogen atoms.
[28]G. A. Petersson, S. Zhong, J. A. Montgomery, and M. J. Frisch, J. Chem. Phys. **118**, 1101 (2003).
[29]H. J. F. Jansen, Phys. Rev. B **38**, 8022 (1988).
[30]H. Kornfeld, Z. Phys. **22**, 27 (1924).
[31]C. K. Lo, J. T. K. Wan, and K. W. Yu, J. Phys. Condens. Matter **13**, 1315 (2001).
[32]A. Grzybowski, E. Gwóźdź, and A. Bródka, Phys. Rev. B **61**, 6706 (2000).
[33]R. S. Mulliken, J. Chem. Phys. **23**, 1833 (1955).
[34]H. J. Monkhorst and J. D. Pack, Phys. Rev. B **13**, 5188 (1976).
[35]M. Methfessel and A. T. Paxton, Phys. Rev. B **40**, 3616 (1989).
[36]H. T. Jeng and D. S. Wang, J. Magn. Magn. Mater. **317**, 46 (2007).
[37]C. L. Fu and A. J. Freeman, Phys. Rev. B **35**, 925 (1987).
[38]R. Pentcheva and M. Scheffler, Phys. Rev. B **65**, 155418 (2002).
[39]X. Wang, D. Wang, R. Wu, and A. J. Freeman, J. Magn. Magn. Mater. **159**, 337 (1996).
[40]V. M. Karpan, G. Giovannetti, P. A. Khomyakov, M. Talanana, A. A. Starikov, M. Zwierzycki, J. van den Brink, G. Brocks, and P. J. Kelly, Phys. Rev. Lett. **99**, 176602 (2007).
[41]C. Vo-Van *et al.*, New J. Phys. **12**, 103040 (2010).
[42]A. Fert and H. Jaffrès, Phys. Rev. B **64**, 184420 (2001).
[43]D. S. Wang, R. Wu, and A. J. Freeman, Phys. Rev. Lett. **70**, 869 (1993).
[44]R. Shimabukuro, K. Nakamura, T. Akiyama, and T. Ito, Physica E **42**, 1014 (2010).
[45]H. J. G. Draaisma and W. J. M. de Jonge, J. Appl. Phys. **64**, 3610 (1988).
[46]D. Hobbs and J. Hafner, J. Phys. Condens. Matter **12**, 7025 (2000).
[47]H. L. Meyerheim *et al.*, Phys. Rev. Lett. **103**, 267202 (2009).
[48]B. Y. Yavorsky, P. Zahn, and I. Mertig, Phys. Rev. B **70**, 014413 (2004).
[49]B. Stärk, P. Krüger, and J. Pollmann, in *Proceedings of NIC Symposium* (von Neumann Institute for Computing, FZ-Jülich, 2010), p. 207.
[50]C. Kittel, *Introduction to Solid State Physics*, 2nd ed. (Wiley, New York, 1965).